Tunable high-Q tapered silica microcylinder filter

Chenglong Yin (阴成龙), Jinyi Gu (顾进益), Mi Li (李 密), and Yuejiang Song (宋跃江)*

Institute of Optical Communication Engineering, Nanjing University, Nanjing 210093, China

**Corresponding author: yjsong@nju.edu.cn*

Received March 20, 2013; accepted May 13, 2013; posted online July 26, 2013

We propose and demonstrate a tunable optical filter based on a tapered silica microcylinder, whose diameter is gradually varied along its longitudinal axis. The tapered microcylinder comprises a slowly varying transition zone fabricated through the fiber drawing technique. Given the tapered diameter of the microcylinder, the resonant wavelengths can be tuned by displacing the tapered microcylinder. This tunable filter exhibits a high Q-factor ($\sim 10^6$) and a large tuning range (>1 free spectral range (FSR)).

OCIS codes: 230.7408, 230.3990, 230.4685, 230.5750.

doi: 10.3788/COL201311.082302.

Optical microcavities with high-Q whispering gallery modes (WGMs) have elicited extensive interest for numerous photonic applications[1−5]. Precisely tuning the resonant WGMs of optical microcavities is important for practical applications. The WGM microcavity is a morphology-dependent resonator. It is rigidly determined by the profile and optical permittivity of the microcavity. In principle, therefore, any change in profile or optical permittivity tunes the WGM. For example, WGMs can be tuned by changing microsphere size through chemical etching[6] or by changing the shapes of microcavities through externally applied tension or pressure[7−9]. The resonant WGM can also be tuned by modifying the refractive index of microcavity media ($LiNbO_3$ crystal, semiconductor, liquid crystal, etc.) through the electro-optic effect[10−12]. Both the profile and refractive index can also be simultaneously changed through the thermal-optic effect[13−15] to tune the resonant WGM. Each of these tuning methods has advantages and disadvantages. Chemical etching or applied forces may achieve a wide tuning range but suffer from low repeatability or are unsuitable for large volumes. Tuning through electrical methods is convenient for compacting and integrating components but presents difficulties in realizing large tuning ranges and compatibility with fibers.

In this letter, we propose and demonstrate a new mechanically tunable tapered microcylinder resonator with a diameter that is tapered very slowly along its longitudinal direction. The tapered microcylinder is fabricated from the slowly varying transition zone of the drawn fiber. When the microresonator is displaced along its longitudinal axis, different WGM wavelengths can be excited and tuned because of the slowly varying diameter of the microcylinder resonator. This tapered microcylinder-based optical filter not only has wide tuning ranges (greater than 1 free spectral range (FSR)) but also exhibits a high Q-factor ($\sim 10^6$) and coupling efficiency ($\sim$90%) during the entire course of tuning.

Figure 1(a) shows the schematic of the tunable tapered microcylinder filter. The fiber is tapered with a $\sim$2-μm diameter, fixed onto fiber clampers, and kept perpendicular to the tapered microcylinder. The fiber is used for optical coupling with the microcavity. The tapered microcylinder with a diameter that is slowly varied along the longitudinal axis is used as the cylindrical resonator. This microcylinder is fixed onto a stage and can be precisely displaced back and forth. The WGM states of the microcylinder resonator can be excited using a fiber taper, as illustrated in Fig. 1. Given that the round-trip phase change of the optical resonances along the cross-section surface must be an integer that is a multiple of 2π, the wavelengths can be approximately predicted as[16] $\lambda = \pi n D/m$, where D is the diameter of the local states, n is the effective refractive index, and the integer above m is the angular mode number. We focus on the relationship between the WGM resonant wavelength and varying diameter. Resonant wavelength is approximately proportional to diameter. Different local states are excited when the fiber taper is coupled with the tapered microcylinder at a different diameter (Fig. 1(a)). The resonant wavelength can be tuned if the fiber taper is coupled with microresonators with different diameters by simply displacing the tapered microcylinder (Fig. 1(b)) because the WGMs are highly dependent on microcylinder morphology.

Given the resonant modes on the cross-section plane, we approximately calculate the shift in resonant wavelength with diameter by referring to Mie theory[17]. Two types of polarizations exist: the TE and TM modes, whose electric fields are parallel and perpendicular to the longitudinal direction, respectively. The resonant wavelength can be calculated by matching the boundary conditions of the electromagnetic field. The shift in TM

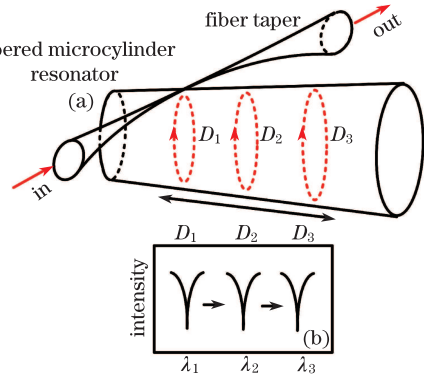

Fig. 1. (a) Schematic of the tunable tapered microcylinder filter. (b) WGM spectral shift with different diameters.

resonant wavelength with the diameter of the resonant modes on the cross-section plane for the silica cylindrical microcavity is calculated and shown in Fig. 2. In our calculation, the refractive indexes of silica and air are 1.444 and 1.000, respectively. The variations in effective diameter range from 86.40 to 86.76 μm, which corresponds to the experimental range. Mode number $m = 244$ and $l = 1, 2$ are calculated, which correspond to the resonant wavelength near the 1.55-μm waveband. Figure 2 shows that each WGM has an approximately linear wavelength shift with diameter at different modes. Radial modes $l = 1$ and $l = 2$ have slightly different wavelength shift slopes, i.e., 17.84 and 17.23 nm/μm, respectively. The TE and TM polarization modes also have the same shift slope for the same (m, l). The dispersion in simulation can be disregarded because only a narrow wavelength range (<10 nm) is considered.

The tapered microcylinder resonator is fabricated through the fiber drawing technique. The standard single-mode fiber fixed onto a couple of motorized stages is drawn while being heated using a stable hydrogen flame (Fig. 3(a)). We can achieve the expected slowly varying transition zone between the drawn fiber and the original fiber by carefully controlling the parameters of the feed and draw speeds of two stages and heating zone length[18]. The original diameter D_0 of the fiber gradually decreases to the drawn diameter D_1 through the fabrication. In our experiment, the feed and draw speeds are 20 and 40 μm/s, respectively. The heating zone of the flame is ~3 mm, and the drawn length of the draw stage is 20 mm. The image of the slowly varying transition zone is shown in Fig. 3(b). The original diameter D_0 of the fiber is 125 μm. The drawn diameter D_1 is 86.4 μm, which is governed by the conversion of mass. The length

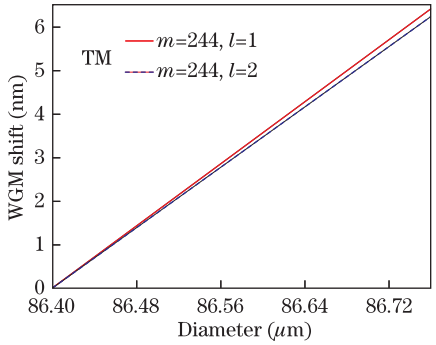

Fig. 2. (Color online) WGM resonant wavelength shift with the effective diameter of the resonant modes on the cross-section plane.

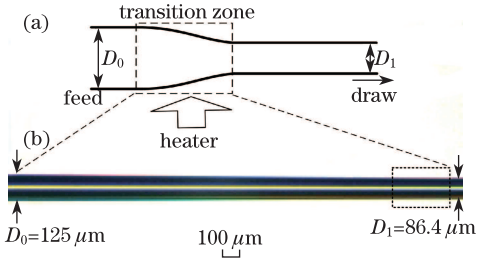

Fig. 3. (Color online) (a) Schematic of the tapered silica microcylinder fabrication. (b) Microscopic image of the tapered silica microcylinder. The dashed box shows the tunable microcylinder resonator used in the experiment.

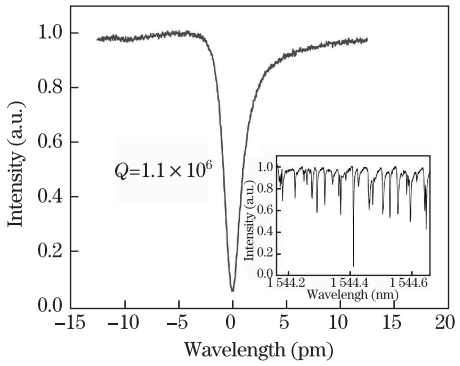

Fig. 4. (Color online) WGM spectrum with a central wavelength of 1544.4115 nm. Inset: broadband WGMs in the ~1544.4-nm band.

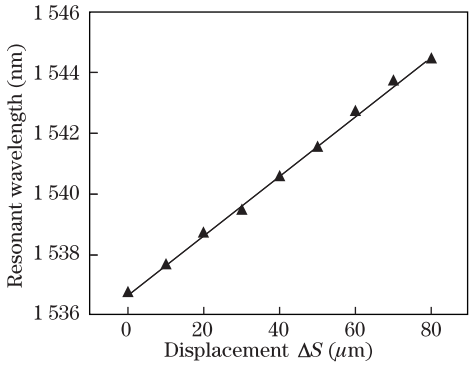

Fig. 5. (Color online) Resonant wavelength shift of the tapered microcylinder resonator under different displacements.

of the entire transition zone is ~2.1 mm. The longitudinal variation in the diameter of the silica cylinder is clearly observed using a video microscope with a 1-μm resolution. The slowly varying transition zone near the drawn fiber shown in the dashed box of Fig. 3(b) is used as the tapered microcylinder resonator in our experiment because of the minimum slope of the zone.

Figure 2 shows that WGM wavelength highly depends on microcavity diameter. To tune the resonant wavelength within one FSR (~6.3 nm), only the 0.36-μm diameter deviation is considered. We choose a length of the silica microcylinder as shown in the dashed box of Fig. 3(b) to test resonant characteristics. The fiber taper is used to excite the WGMs in the tapered microcylinder resonator and is kept naturally touching the tapered cylinder throughout the experiment. The WGM properties of the cylindrical microresonator are characterized by the transmission spectrum of the fiber taper coupled microcylinder. To obtain the transmission spectrum, the tunable narrow linewidth (~200 kHz) laser in the 1 550-nm band is scanned and input into the fiber taper; the output laser is detected using a photodetector and monitored on an oscilloscope. Figure 4 shows a typical WGM spectrum of the microcylinder resonator: it has a central wavelength of ~1 544.42 nm, corresponding to m~244, a loaded Q-factor of ~1.1×10^6, and a coupling efficiency of ~95%. The broadband WGM spectra (1 554.2–1 554.6 nm) are shown in the inset of Fig. 4.

The WGMs of the microresonator can be precisely tuned by carefully Ldisplacing the tapered silica microcylinder fixed onto a stage with a 1-μm resolution. As the displacement ΔS of the microcylinder is adjusted,

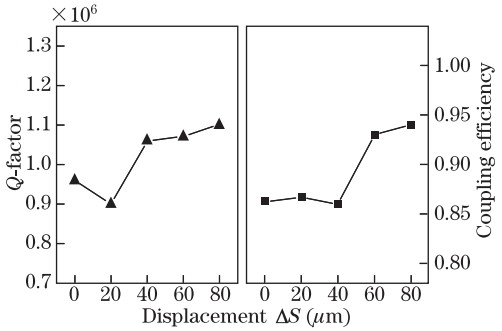

Fig. 6. Q-factor and coupling efficiency in the tuning process.

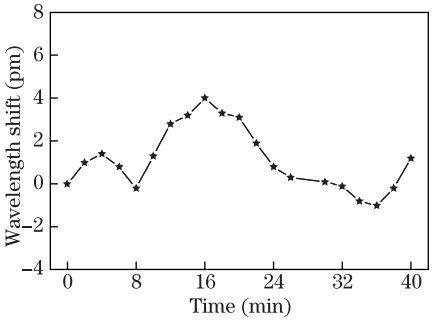

Fig. 7. Wavelength stability of the resonant filter in 40 min.

the fiber taper excites the WGM of the microcylinder resonator with different diameters D to continuously tune the resonant wavelength. Figure 5 shows that the resonant wavelength shift of the tapered microcylinder is approximately proportional to the displacement ΔS with a 95.86-pm/μm slope, indicating the linearly varying profile of the tapered microcylinder in the displacement range. The tuning range is ~7.68 nm for the total 80-μm displacement, indicating a ~0.44-μm effective diameter variation within this displacement range (see calculated slope in Fig. 2). A larger tuning range is achieved with the further displacement of the tapered microcylinder in our experiment. Wavelength filtering can be realized in any wavelength with such a tapered microcylinder filter because the tuning range is greater than 1 FSR of this microcylinder. One-fiftieth of the WGM linewidth is assumed to be the detectable wavelength shift in our experiment[19]; thus, this microcylinder tunable filter has a wavelength resolution of ~0.028 pm. The Q-factor and coupling efficiency of the tapered microcylinder filter are also studied and depicted in Fig. 6. The Q-factor and coupling efficiency vary between $(0.85–1.1)\times 10^6$ and 85% – 95% respectively, and remain at almost stable high values.

The wavelength stability of the microcylinder resonator, which is placed in air without temperature control and with vibration isolation, is measured at a time interval of 2 min (Fig. 7). The maximum wavelength fluctuation is 5 pm at an interval of 40 min. The wavelength derivation contributes to ambient temperature fluctuations. Therefore, precise temperature control is necessary in practical applications to reduce the instability of resonant wavelength.

In conclusion, a tunable optical filter based on a tapered silica microcylinder is demonstrated. The slowly varying transition zone fabricated through the fiber drawing technique is used as the microcylinder resonator. The WGM resonant wavelength can be tuned by displacing the microcylinder because of the varying diameters of the microcylinder. In the experiment, a wavelength tuning slope of 95.86 pm/μm is attained while preserving a high Q-factor and coupling efficiency. The ideal spectral resolution of the resonant filter reaches 0.028 pm, and the wavelength can be tuned in any waveband. As a mechanical tuning scheme, the proposed filter may have a weaker response speed than that of electrically tunable filters.

This work was supported by the National Natural Science Foundation of China (Nos. 60907022 and 61205045) and the National Natural Science Foundation of Jiangsu Province (No. BK2011555).

References

1. K. J. Vahala, Nature **424,** 839 (2003).
2. V. S. Ilchenko and A. B. Matsko, IEEE J. Quantum Electron. **12,** 15 (2006).
3. C. Dong, C. Zou, J. Cui, Y. Yang, Z. Han, and G. Guo, Chin. Opt. Lett. **7,** 299 (2009).
4. Y. D. Yang, Y. Z. Huang, and Q. Chen, Phys. Rev. A **75,** 013817 (2007).
5. J. Teng, J. Feng, J. Guo, and M. Zhao, Chin. Opt. Lett. **10,** S21304 (2012).
6. I. M. White, N. M. Hanumegowda, H. Oveys, and X. Fan, Opt. Express **13,** 10754 (2005).
7. M. Pöllinger, D. O'Shea, F. Warken, and A. Rauschenbeutel, Phys. Rev. Lett. **103,** 053901 (2009).
8. V. S. Ilchenko, P. S. Volikov, V. L. Velichansky, F. Treussart, V. Lefèvre-Seguin, J. -M. Raimond, and S. Haroche, Opt. Commum. **145,** 86 (1998).
9. T. Ioppolo and M. V. Otugen, J. Opt. Soc. Am. B **24,** 2721 (2007).
10. A. A. Savchenkov, V. S. Ilchenko, A. B. Matsko, and L. Maleki, Electron. Lett. **39,** 389 (2003).
11. K. Djordjev, S. J. Choi, S. J. Choi, and P. D. Dapkus, IEEE Photon. Technol. Lett. **14,** 828 (2002).
12. M. Humar, M. Ravnik, S. Pajk, and I. Musevic, Nature Photon. **3,** 595 (2009).
13. D. Armani, B. Min, A. Martin, and K. J. Vahala, Appl. Phys. Lett. **85,** 5439 (2004).
14. H. C. Tapalian, J. P. Laine, and P. A. Lane, IEEE Photon. Technol. Lett. **14,** 1118 (2002).
15. F. Monifi, J. Friedlein, S. K. Ozdemir, and L. Yang, J. Lightwave Technol. **30,** 3306 (2012).
16. T. A. Birks, J. C. Knight, and T. E. Dimmick, IEEE Photon. Technol. Lett. **12,** 182 (2000).
17. C. F. Bohren and D. R. Huffman, *Absorption and Scattering of Light by Small Particles* (John Wiley & Sons, New York, 1998).
18. U. C. Paek and R. B. Runk, J. Appl. Phys. **49,** 4417 (1978).
19. S. Arnold, M. Khoshsima, I. Teraoka, S. Holler, and F. Vollmer, Opt. Lett. **28,** 272 (2003).